Optimal Sensor Placement: a sensor density approach[1]

D. Tcherniak [1]
[1] Hottinger Brüel & Kjær,
Teknikerbyen 28, 2830 Virum, Denmark
e-mail: **dmitri.tcherniak@hbkworld.com**

Abstract

Finding the optimal number and location of measurement points for modal tests and virtual sensing applications is a non-trivial task. The numerical mode shapes of the test object, if available, can assist in picking the optimal sensor number and locations. As in any optimization problem, an objective function is formulated. The typical objective functions are the determinant of the Fisher Information Matrix, the sum of the off-diagonal elements of the AutoMAC matrix, the condition number of the mode shape matrix, etc. The optimization problem is posed as distributing the given number of sensors in the candidate locations to maximize (or minimize) the chosen objective function. This binary optimization problem is typically solved by using sequential sensor placement or genetic algorithms. This study suggests the relaxation of the binary optimization problem by introducing sensor density: in each candidate location, the sensor is allowed to have a density varying from 0 (no sensor) to 1 (there is a sensor). In this case, the derivative of the objective function with respect to sensor configuration exists, and powerful gradient-based optimization algorithms can be employed. The study elaborates on the suggested method and demonstrates its advantages in application to test objects of different complexity.

1 Introduction

When planning a campaign for structural dynamics measurements, it is always a task to find the optimal number and location of measurement points. A common practice is to place a sufficient number of measurement points in a fashion that generates a regular mesh on the test object [1]. The wireframe model, built on top of the mesh, allows the test engineer to animate the operational deflection shapes and mode shapes in a subjectively easy to comprehend way. If the number of measurement points exceeds the number of available sensors, the sensor roving technique is employed: the available sensors are consequently moved between the desired locations, thus the sensors shortage is compensated by the extended measurement time. This approach is acceptable for in-situ and lab measurements, where the typical tasks are troubleshooting and numerical model validation.

In the last decade, the increased availability of sensors, measurement channels, and data processing/storage capacities made the permanent vibration monitoring of civil and mechanical structures feasible. In this scenario, the sensors are permanently installed on the structure, and the data acquisition takes place during the entire life of the structure. The main applications of vibration monitoring were structural health monitoring (SHM) and condition monitoring (CM). More recently, following the overall digitalization trend, vibration monitoring becomes an element of the digital twin (DT) concept, where, for example, the virtual sensing methods provide the input to the fatigue evaluation algorithm and can be used for estimating the remaining lifetime of the structures.

It is important to note the key difference between laboratory measurements and vibration monitoring. In the former case, *only one* "instance" of the test object is *only* thoughtfully tested *once*. This can justify a big, often redundant, number of measurement points placed in the nodes of a regular mesh. In the case of

[1] Submitted to *International Conference on Noise and Vibration Engineering* (ISMA), Leuven, Belgium, 2022.

vibration monitoring, *all* manufactured units of the test object are monitored during their *entire* lifetime. The measurement point redundancy is not economically justifiable in this case, and the minimum necessary number of sensors must be used, and they need to be placed at the optimal locations.

The problem of optimal sensor placement (OSP) in structural dynamics was postulated in 1991. Kammer [2] introduced the problem and established the classical OSP formulation: based on numerical mode shapes (for example, those resulting from a FE model), by selecting "a given number of sensor locations from an initial much larger set" to maximize some *utility* of the measurement system. It was also noted that the OSP problem consists of two challenges:

1) Which utility to choose.

2) How to solve the binary (also known as *discrete*, *boolean*, and *combinatorial*) optimization problem.

Objective function. To answer the first question, one must refer to the application, namely, the purpose of the measurement system. During the three decades since the OSP problem postulation, all the above-mentioned structural vibration applications were attempted from the OSP viewpoint, and a vast number of studies were published; a few are mentioned below: Kammer in [2] considered the experimental validation of the FE model. Shih *et al.* [3] concerned the OSP to improve the modal identification. C. Papadimitriou made a significant contribution to the generalization of the OSP in application to wide-ranging parametric system identification problems, for example, [4], [5]. In [6], Mendler *et al.* optimized the sensor locations to increase damage detectability for statistical damage detection. Other OSP formulations for SHM were reviewed in [7]. The OSP for virtual sensing applications was studied in [8], [9], where the latter paper also took the sensors' installation cost into considerations.

Optimization method. The second OSP challenge is *how* to solve the optimization problem. The difficulty is that the optimization problem is binary: in any possible sensor location, there should be either a sensor or no sensor, that is, the design variable at each possible sensor location i is $\delta_i = \{0;\ 1\}$. It means in mathematical terms that the objective function is not a continuous function of the sensors' distribution, its gradient w.r.t. the latter does not exist, and fast gradient-based optimization algorithms cannot be applied to this case. Different approaches were suggested to solve this problem. The exhaustive search (also known as a brute-force method), where all possible sensor configurations are attempted, is not applicable as the number of the possible combinations is astronomic even for small-size problems. When introducing the OSP problem in [2], Kammer also suggested the algorithm for solving the optimization problem. Starting from the full sensor configuration, where the sensors are placed at all possible locations, the algorithm sequentially, one by one, removes the sensor that contributes least to the objective function. Later, this approach was generalized by Papadimitriou, [10], who also introduced the term "sequential sensor placement" (SSP) and suggested two SSP types: BSSP (backward SSP) and FSSP (forward SSP). As the name suggests, the latter approach starts from a not instrumented test object and one by one adds a sensor to the locations where it contributes most to the objective function. Study [9] suggested a combination of the FSSP and BSSP techniques. The same study demonstrated a good performance of the SSP methods, exemplifying this by comparing the SSP with the results of the exhaustive search on a relatively small OSP problem. Kim and Park in [11] suggested a way to reduce the number of iterations that BSSP needs to converge to an optimal solution and thus boost the performance of the technique.

Though the SSP-related methods are efficient and demonstrate good performance, they cannot guarantee to find a global optimum of the objective function due to their sequential nature. In this sense, the genetic algorithms (GA, also known as evolutionary algorithms) are an alternative to SSP. Since the first application of GA to the OSP problem in [12], GA has successfully competed with SSP in OSP (for example, [13], [14]).

Both SSP- and GA-based OSP can be extended to multi-objective optimization via the Pareto approach, [15]. In this case, several objective functions can be mixed, and the algorithm will be able to capture several optimal points along the Pareto front.

The present study employs a different, *relaxed* optimization approach: instead of the binary formulation $\delta_i = \{0;\ 1\}$, we introduce the *sensor density*, which can continuously vary from zero (no sensor) to one (there is a sensor): $\rho_i = [0;\ 1]$. This approach was inspired by the achievements in topology optimization (for example, **www.topopt.dtu.dk**) where the binary relaxation is employed for designing lightweight

structures and mechanisms with given static and dynamic properties. It turned out that the relaxation approach has already been applied to the OSP problem; it was introduced in [16] under the name *convex optimization* and applied to OSP for SHM in [17] and to Bayesian OSP in [18].

The presented paper is thought to represent a practicing test engineer's view on the OSP. Assuming the mode shapes are available from the FE analysis, it applies the BSSP and the senor density approach first to a simple structure (a rectangular plate) and then to a typical 3D test object. The numerical mode shapes for the latter test object are defined at about 24,000 nodes. The paper also addresses the choice of the optimal *number* of sensors and the use of monoaxial sensors on 3D structures, focusing on their orientation. These issues, though their practical importance, are often ignored in the OSP literature. Finally, the paper demonstrates the application of the sensor density approach in more traditional engineering formulations such as reducing the correlation between the modes (minimization of the off-diagonal elements of the AutoMAC matrix) and solving the inverse problem. The latter is a common task in some engineering tools for example, the orthogonality check.

2 Theoretical background

The presented study employs the objective function introduced in [2] and the paragraphs below briefly describe it following its interpretation given in [5] for the binary formulation and then extend it to the sensor density formulation.

Let us assume $\mathbf{\Phi} \in \mathbb{R}^{N\times M}$ is a mode shape matrix built of M mode shape vectors defined at N degrees-of-freedom (DOFs) and matrix $\mathbf{L} \in \mathbb{N}^{N_o\times N}$ is the *observation matrix*, where N_o is the number of the observed DOFs. Matrix $\mathbf{L}$ is comprised of zeros and ones and can be constructed from the sensor configuration vector $\boldsymbol{\delta} \in \mathbb{N}^{N\times 1}$ with elements $\delta_i = 1$ at the observed DOFs and $\delta_i = 0$ otherwise, [4]. The matrix is constructed in such a way that the product $\mathbf{L\Phi} \in \mathbb{R}^{N_o\times M}$ provides the mode shape vectors at the observed DOFs and $diag(\mathbf{L}^T\mathbf{L}) = \boldsymbol{\delta}$. The Fisher Information Matrix (FIM) is defined as

$$\mathbf{Q} = (\mathbf{L\Phi})^T(\mathbf{L\Sigma}_\mathrm{t}\mathbf{L}^T)^{-1}(\mathbf{L\Phi}), \tag{1}$$

where $\mathbf{\Sigma}_\mathrm{t}$ is the covariance matrix of the prediction error. Following Kammer [2], Papadimitriou [19], [4] introduced the information entropy norm as the measure of the uncertainty in the experimental model parameter estimation and showed that the information entropy depends on the determinant of FIM. He also proved the important proposition implying that "the information entropy reduces as additional sensors are placed in a structure", [4]. It was proven that minimizing the uncertainty in the experimental model parameter estimation is equivalent to maximizing the determinant of FIM. Thus, the determinant of FIM is a popular objective function in OSP, and BSSP and GA are the popular algorithms to find the optimal sensor configuration maximizing it.

The presented study employs the same objective function; however, it assumes that the sensors are placed in *all* possible DOFs of the structure: $\mathbf{L} = \mathbf{E}^{N\times N}$, and each sensor is assigned with the sensor density ρ_i that can vary between 0 and 1: $\rho_i = [0; 1]$. The sensor densities are organized in a vector $\boldsymbol{\rho} \in \mathbb{N}^{N\times 1}$. The density defines the *sensing ability* of a sensor by affecting its measurement uncertainty and thus affects the $\mathbf{\Sigma}_\mathrm{t}$ matrix. It is assumed that $\mathbf{\Sigma}_\mathrm{t} = \mathbf{P}^{-2}$, where $\mathbf{P} = diag(\boldsymbol{\rho})$. For $\rho_i = 1$, the corresponding element of the $\mathbf{\Sigma}_\mathrm{t}$ matrix is 1 and for small values of ρ_i the corresponding sensor measurement uncertainty is a big number. These considerations yield

$$\mathbf{Q} = \mathbf{\Phi}^T\mathbf{P}^2\mathbf{\Phi}. \tag{2}$$

It is easy to show that in the limit case, when ρ_i takes only 0 or 1 values, the FIM computed via (2) is the same as via (1) (assuming $\mathbf{\Sigma}_\mathrm{t} = \mathbf{E}$).

The considered optimization problem that should lead to the optimal sensor configuration $\boldsymbol{\rho}^*$ is formulated as:

$$\boldsymbol{\rho}^* = \underset{\boldsymbol{\rho}}{\mathrm{argmax}}(\det(\mathbf{Q})) \tag{3}$$

subject to

$$\rho_i \in [0;1]$$

$$\mathbf{1}^T\boldsymbol{\rho} \leq C$$

The last constraint limits the amount of sensing to be distributed, though in the final designs it is not necessary that $N_o = C$. The list of the constraints can be extended by the application-specific constraints, which will be discussed later.

As $\det(\mathbf{Q})$ is now a function of the continuous variables $\boldsymbol{\rho}$, it is possible to analytically derive its sensitivities w.r.t. $\boldsymbol{\rho}$. It is convenient to present the determinant of $\mathbf{Q}$ as the product of its eigenvalues $\lambda_m, m = 1..M$:

$$\det(\mathbf{Q}) = \prod_{m=1}^{M} \lambda_m, \tag{4}$$

and the derivatives of the eigenvalues w.r.t. $\boldsymbol{\rho}$ are readily available.

Efficient gradient-based optimization routines can now be employed; in the examples considered below, the method of moving asymptotes (MMA) [20] was used.

The optimization starts with even distribution of the available amount of sensing to all DOFs: $\rho_i = C/N$, thus the constraints in (3) are fulfilled. Normally, the algorithm converges to the solution with sensor densities being ones and zeros. In some cases, when additional application-specific constraints are involved, the sensor densities may have intermediate values between 0 and 1. Then, the final sensor system design $\rho_i^{(fin)}$, $i = 1..N$, is formed by applying a threshold ρ_{thr}:

$$\rho_i^{(fin)} = \begin{cases} 0, & \rho_i < \rho_{thr} \\ 1, & \rho_i \geq \rho_{thr} \end{cases} \tag{5}$$

This manipulation may cause a slight difference between the values of the objective function and the constraint of the final design and those observed during the optimization process.

3 Application to a simple mechanical system

A freely supported uniform rectangular plate with the ratio of the long and short side 40/27 was modeled in a FE software, and the first 10 flexural mass-matrix normalized mode shapes were obtained. Only the DOFs normal to the plate surface were considered, and the dimension of the mode shape matrix was 3974×10. The mode shapes were input to the two OSP algorithms: BSSP (implemented in HBK's BK Connect® software) and the presented sensor density-based algorithm. The resulting sensor configurations are presented in Figure 1.

It appears that the two OSP algorithms generate almost identical 12-sensor designs, though the BSSP produces the one with a slightly better objective function value. For comparison, a regular 4×3 sensors configuration is shown as well, it is characterized by 50 times lower objective function and some inferior off-diagonal term of the AutoMAC matrix.

It must be noted that the optimization formulation (3) does not involve any optimization for AutoMAC, however, a reasonable AutoMAC matrix is a typical side effect of the uncertainty minimization pursued by (3). The formulation (3) can be extended to pursue a better AutoMAC by adding a corresponding constrain, which will be discussed later.

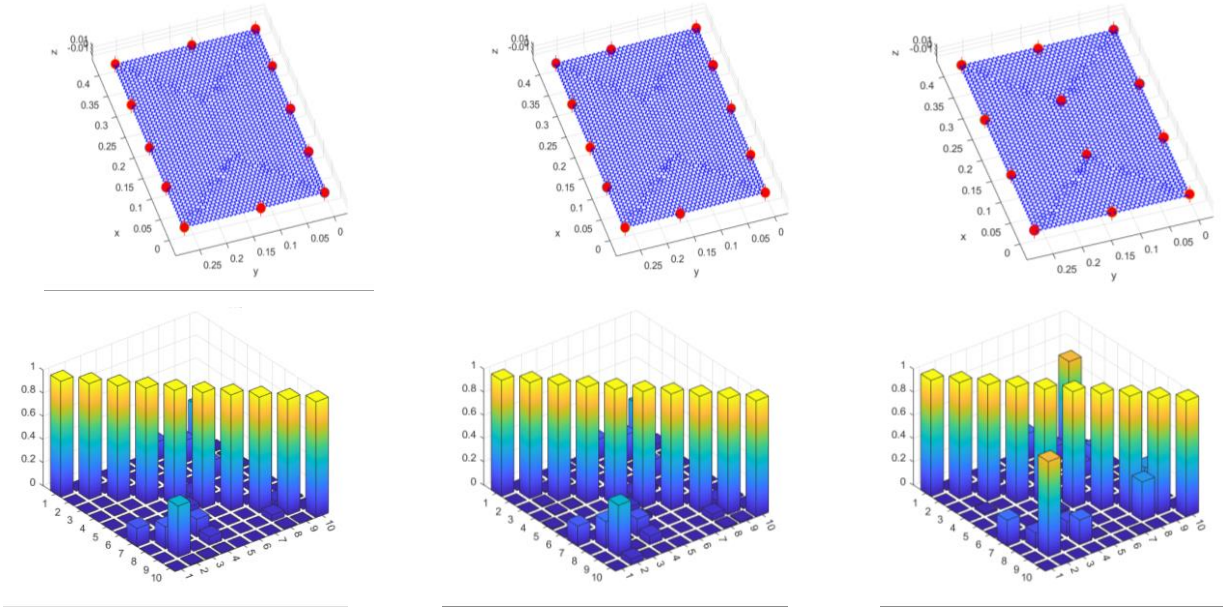

Figure 1: Optimized sensor configurations and the corresponding AutoMAC. Left: BSSP; middle: sensor density approach; right: regular mesh

4 Application to a 3D structure

To demonstrate the algorithms on a more realistic test object, a FE model of a 3-dimensional object was generated (Figure 2). Fourteen first numerical mode shapes (displacement, flexural, mass-matrix normalized) defined in three directions in 23851 nodes, forming the mode shape matrix with dimensions 23851×3×14, were input to the two OSP algorithms.

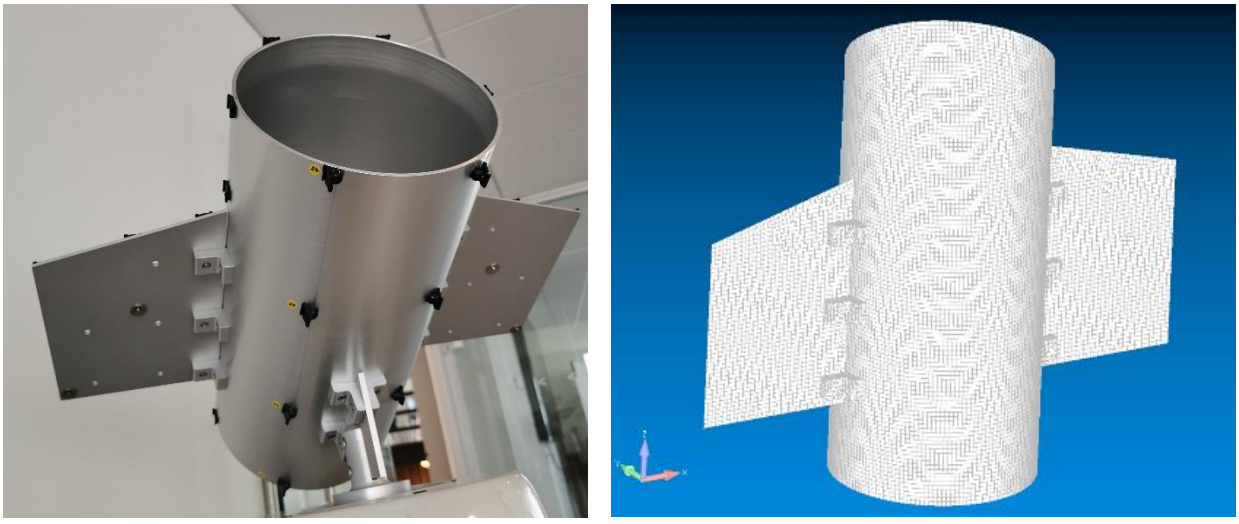

Figure 2: Test object and its FE model (Femap / NX Nastran)

4.1 Placement of triaxial sensors

First, the algorithms were set to find the optimal locations for *triaxial* accelerometers, thus the optimization problem had 23851 design variables: $\boldsymbol{\delta} \in \mathbb{N}^{23851\times1}$ for BSSP and $\boldsymbol{\rho} \in \mathbb{R}^{23851\times1}$ for the sensor density-based algorithms.

The two algorithms generated almost identical configurations comprising 12 triaxial accelerometers (that is, 36 measured DOFs), Figure 3. Only the output of the sensor-density-based algorithm is shown.

4.2 Principal measurement directions

It is evident that some measurement directions are less informative than others. We have utilized this knowledge in the plate example (Section 3), where we retain only the DOFs that are normal to the plate surface. For the second example, the engineering intuition indicates that the Z-direction should be much less informative than the X- and Y-directions and the test engineer could use 12 bi-axial accelerometers instead of triaxial ones, saving 12 measurement channels, without any information loss. However, for complex 3D structures with no apparent mass and stiffness distribution, such intuition-based judgments can be risky.

Below, a simple approach to evaluate the importance of measurement directions is outlined. The approach is based on the principal component analysis of the mode shape matrix. The singular value decomposition (SVD) is applied to the mode shape matrix: the matrix is reformulated as $\boldsymbol{\Phi} \in \mathbb{R}^{N_n\times D\times M}$, where $1 < D \leq 3$ is the spatial dimensionality of the test object, in the considered case $D = 3$ and $N_n$is the number of *nodes* where the sensors can be installed. Then for each node $n = 1 \ldots N_n$, the $D \times M$ matrix $\boldsymbol{\Phi}_n$ is extracted, and SVD is applied to it:

$$\mathbf{U}_n\, \mathbf{S}_n\, \mathbf{V}_n^T = \boldsymbol{\Phi}_n. \tag{6}$$

In the common case when $D \leq M$, the left singular vectors forming the matrix $\mathbf{U}_n \in \mathbb{R}^{D\times D}$ can be considered as a new orthogonal basis defining the *principal measurement directions* (PMD) and the singular values forming the diagonal of $\mathbf{S}_n$ define the scaling of the principal directions. The latter can be used to denote the relative importance of the principal directions. The $\mathbf{U}_n$matrix can also be considered as a rotation matrix that converts the mode shapes $\boldsymbol{\Phi}_n$ to the new principal direction coordinate system, $\boldsymbol{\Phi}_n^{PC} = \mathbf{U}_n\boldsymbol{\Phi}_n$. Figure 4 shows the principal measurement directions for the optimal sensor locations.

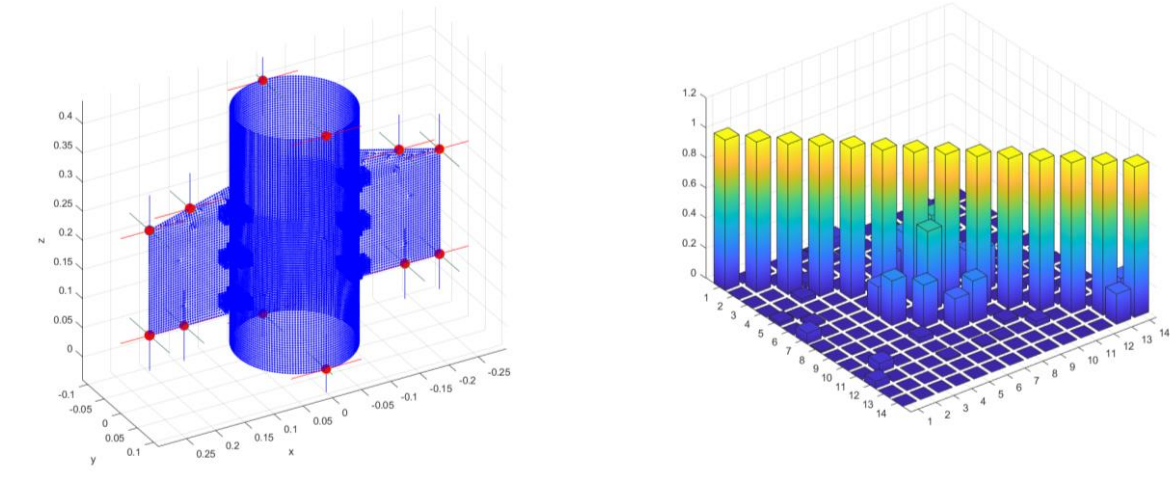

Figure 3: The optimized sensor configuration for triaxial sensors according to the sensor-density approach. The suggested accelerometer positions are shown as red dots and the measurement directions as the red/green/blue lines.

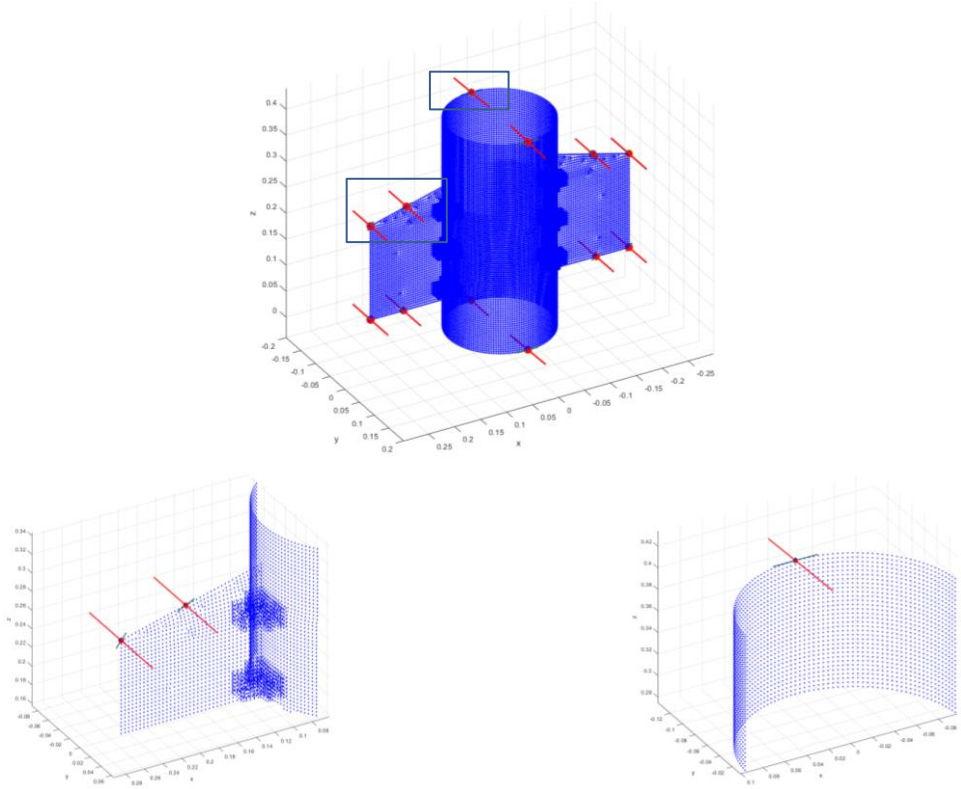

Figure 4: Top: The optimized sensor configuration for triaxial accelerometers. The suggested accelerometer positions are shown as red dots, the measurement directions in the principal coordinates denoted as: red: the first principal direction; green: the second; blue: the third. Bottom insets: zoomed-in views.

It becomes apparent that the first and most important principle measurement directions are close to the vectors that are normal to the "wings" and "body" of the test object. As anticipated, the least important measurement direction is along the Z-axis. Obviously, when looking for the optimal positions of triaxial sensors, the output of the OSP algorithms is not affected by employing or not employing the principal directions. However, the principal directions can be helpful when considering the OSP of monoaxial sensors, which is considered in the following section. It is worth noting that the principal direction concepts can be employed for both BSSP and the sensor-density approach.

4.3 Placement of monoaxial sensors

Though it is more convenient to use triaxial sensors, there are cases where a monoaxial accelerometer is the preferable choice. This is especially the case in vibration monitoring, where the measurement system is permanently installed on the monitored object, and the sensors and measurement channels count defines the economic feasibility of the monitoring system.

In the case of monoaxial sensors, the OSP problem becomes a problem of finding the optimal placement and *orientation* of the sensors (OSP&O). The method considered in the presented study is to exclude the measurement directions from the optimization problem but attach them to some predefined coordinate system(s) (CS), which is often called a measurement CS (MCS). For example, this could be the CS where the mode shapes are defined (which is typically the global CS) or the CS defined by the PMD or some other MCS.

In contrast to the case of triaxial sensors, now we consider all DOFs separately, and thus the optimization problem size increases: $\boldsymbol{\delta} \in \mathbb{N}^{71553\times 1}$ for BSSP and $\boldsymbol{\rho} \in \mathbb{R}^{71553\times 1}$ for the sensor density-based algorithm.

The outputs of the BSSP and the sensor density approaches for different MCS formulations are shown in Figure 5.

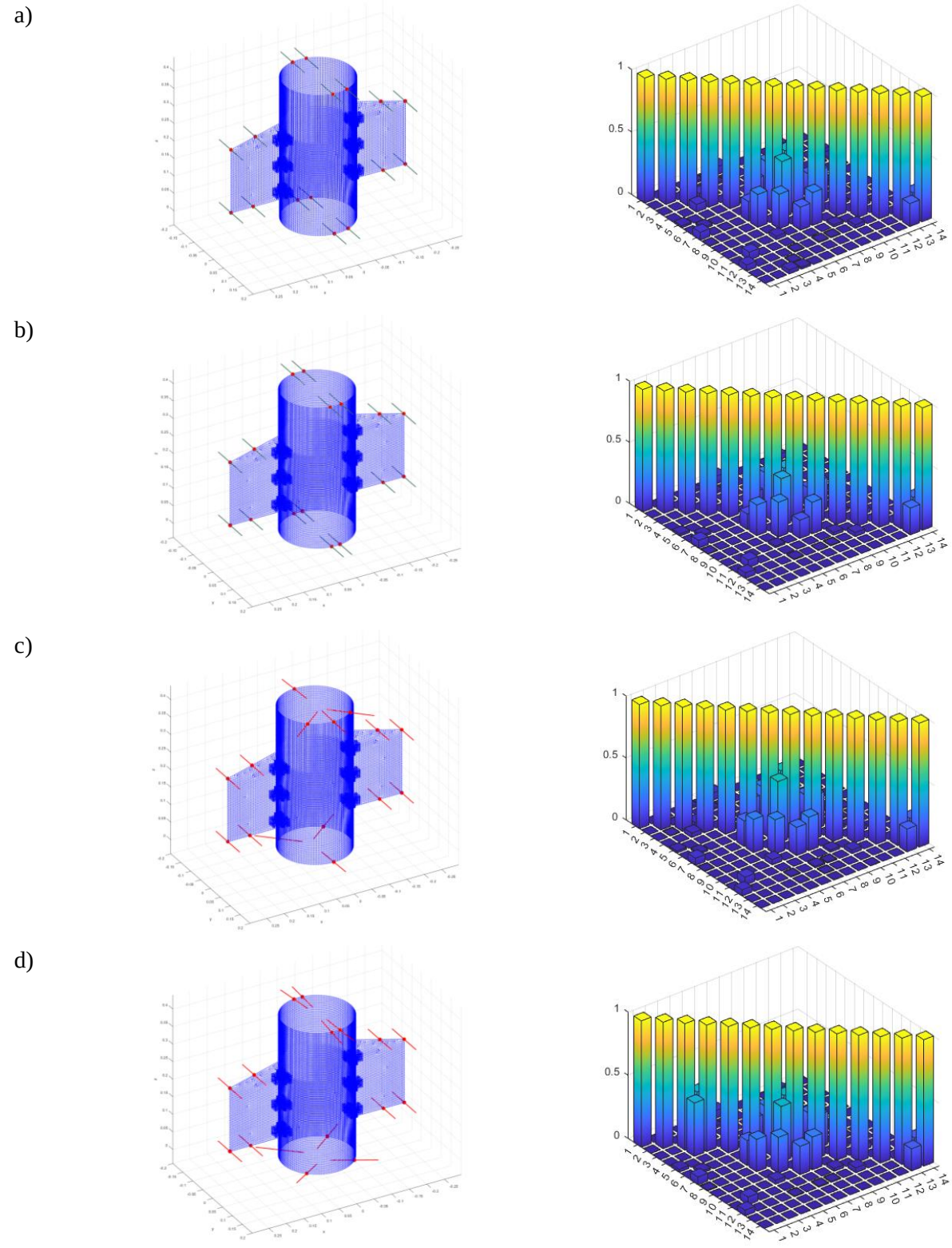

Figure 5: The optimized sensor configuration for monoaxial accelerometers. a) BSSP in global CS; b) sensor-density approach in global CS; c) BSSP in PMD MCS; d) sensor-density approach in PMD MCS.

When the sensor orientation is fixed to match the global CS, the results of both algorithms are slightly counterintuitive (Figure 5a, b): the algorithms suggest using 16 sensors and orienting all of them along the Y-direction. Visually the results are very close, but the resulting objective function is slightly better for the BSSP algorithm.

In the case where the orientation of the sensor is fixed to the PMD, BSSP suggests a 15-sensor design (Figure 5c), and the sensor-density algorithm converges to a 16-sensor configuration (Figure 5d). It is interesting to note that from the resulting objective function perspective, the 15-sensor configuration (Figure 5c) outperforms the 16-sensor ones shown in Figure 5a, b. This does not contradict the proposition proven by Papadimitriou in [4] as the configuration shown in Figure 5c uses the different (and more informative) measurement directions.

The PMD is a valuable indicator of the measurement directions informativity. However, from the practical viewpoint, it might be difficult to mount the sensors according to the PMD. In Figure 6a, the sensor configuration from Figure 5c is shown from the top. It is noticeable that the directions of some sensors mounted on the "body" are not normal to its surface and reproducing the suggested measurement direction in practice will be challenging.

If it is possible to calculate the vectors normal to the test object surface at every node and construct the MCSs based on these vectors, it is practical to use these MCSs for the OSP algorithm. Thus, the mode shapes matrix $\boldsymbol{\Phi}$ in (2) shall be recalculated to transform the mode shapes to the selected MCS. Figure 6c shows the optimized 15 sensors configuration based on such MCSs, Figure 6b is the top view, and Figure 6d the corresponding AutoMAC. The value of the objective function for this configuration is slightly worse compared to the one in Figure 5c, though the designs are very similar.

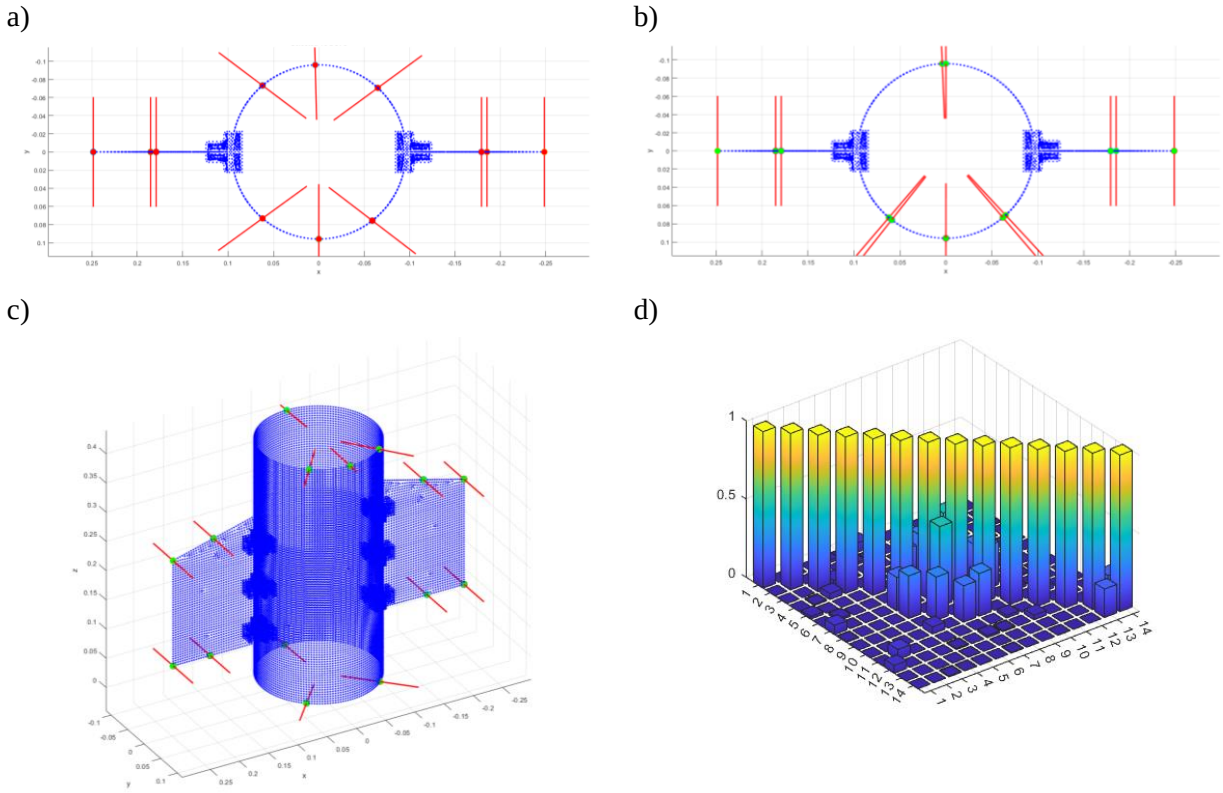

Figure 6: Optimal sensor configurations: a) PMD-based MCSs, top view; b, c, d) flush-mounted sensors: top view, configuration, and AutoMAC, respectively.

a)

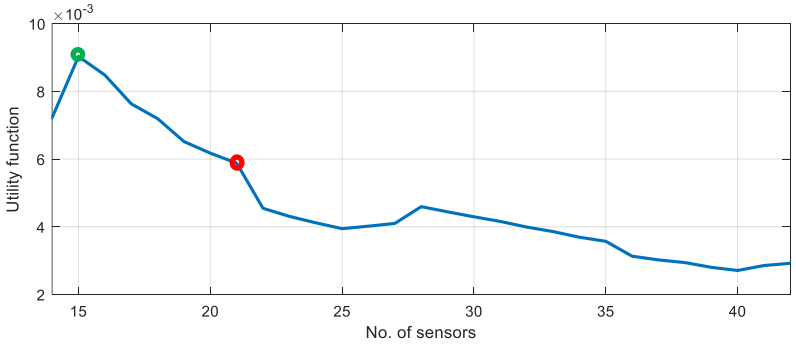

b) c)

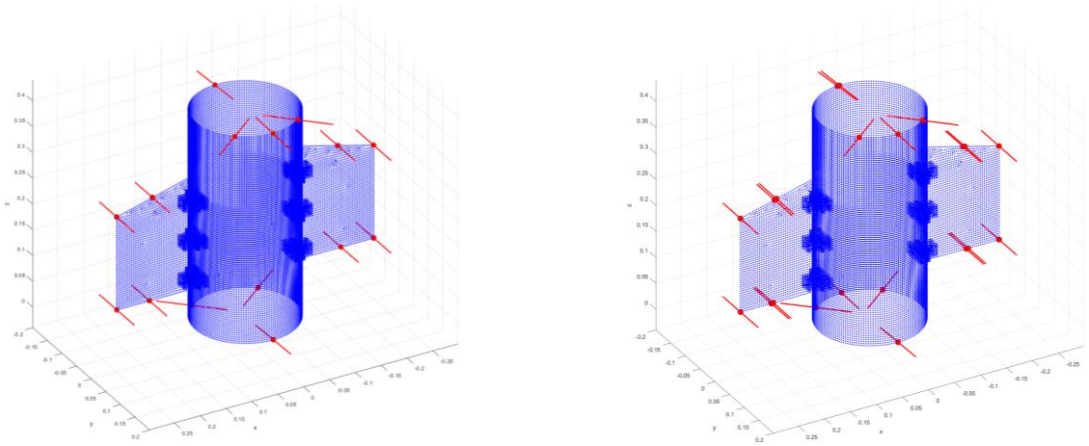

Figure 7: Sensor amount for BSSP. a) The utility function, the dots indicate the two configurations: b) the recommended 15-sensor configuration; c) 21-sensor configuration (sensor clustering).

It is worth noting that the sensor-density approach can logically extend to the OSP&O problem. In this case, the sensor orientation, expressed in the terms of Euler angles or quaternions, can be considered as an extra design variable in addition to the sensor density. This is the field of future research.

5 Notes about the optimal sensor count

The two typical questions a test engineer may ask are: 1) how many sensors I need, and 2) where to place them. The BSSP algorithm does not answer the first question: at each iteration, it produces a sensor configuration and leaves the choice of the optimal one to the user. The sensor-density approach also requires the "available amount of sensing" C as the right-hand side of the last constraint in (3).

For the BSSP-based OSP, the present study suggests an empiric approach, which is based on the following utility function computed at each iteration of BSSP:

$$u^{(i)} = \left(\left(\mathbf{1}^T \boldsymbol{\delta}^{(i)}\right) \kappa\left(\mathbf{L}^{(i)}\boldsymbol{\Phi}\right)\right)^{-1}, \tag{7}$$

where the superscript (i) indicates the iteration and $\kappa(\ldots)$ is the condition number of the argument matrix. The function is the inverse of the product of the condition number of the mode shape vectors at the observed DOFs and the number of the observed DOFs. The usefulness of the condition number as a measure of the utility will be discussed later.

The peak of the utility function indicates the recommended configuration. This approach was employed for all previous illustrations of the BSSP method, and it is implemented in HBK's BK Connect® software. The

utility function computed for the last 28 iterations of the BSSP is shown in Figure 7a followed by two sensor configurations, the recommended one with 15 sensors in Figure 7b and another configuration with 21 sensors, Figure 7c. In general, all configurations with a sensor count greater than 15 are like the recommended one, but instead of placing the sensors in the not instrumented areas, the algorithm tends to "cluster" more sensors around already placed ones (Figure 7c). This "sensor clustering" is a known artifact of the FIM-based objective functions, for example, [21].

The same applies to the sensor-density approach. Selecting a high value of C in (3) leads to sensor clustering. It is recommended to attempt $C = M$ and adjust the value if necessary.

To force the algorithm to place the sensors in the not instrumented areas, it is advisable to increase the number of modes taken into consideration. Figure 8 shows the optimized sensor configurations for M=18, 22 and 24 obtained using the sensor-density approach.

a)

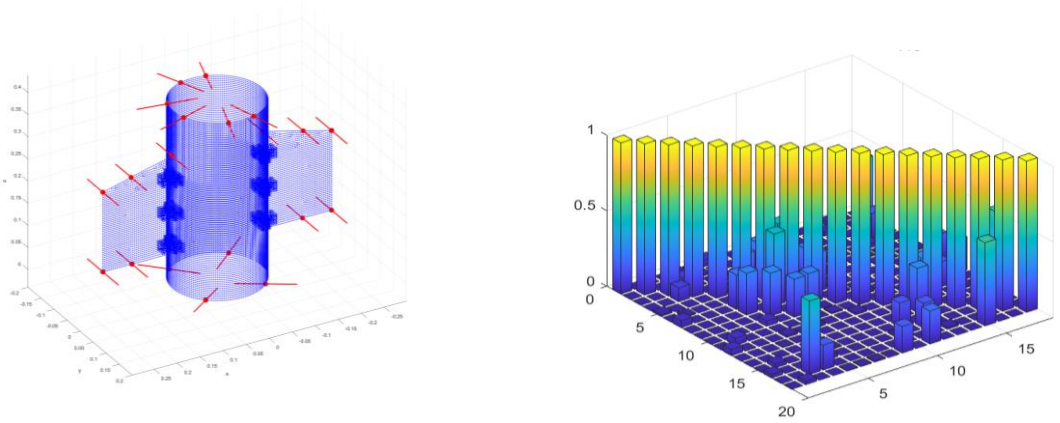

b)

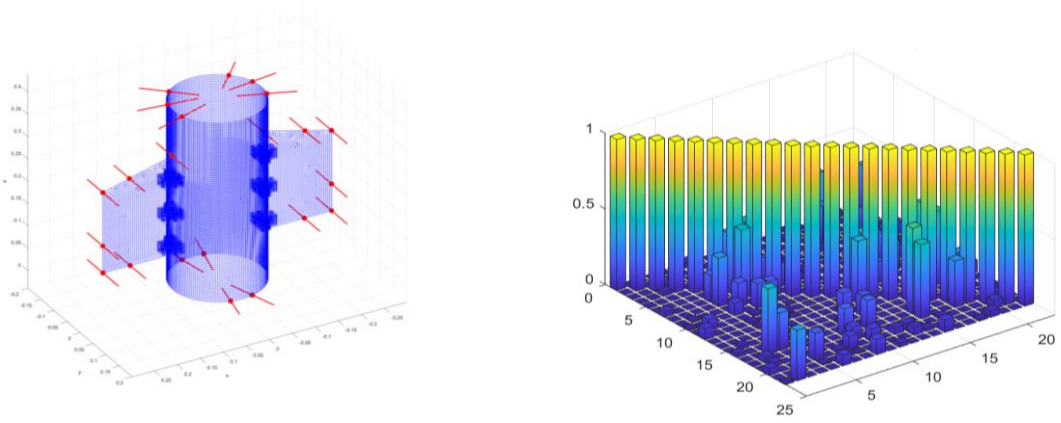

c)

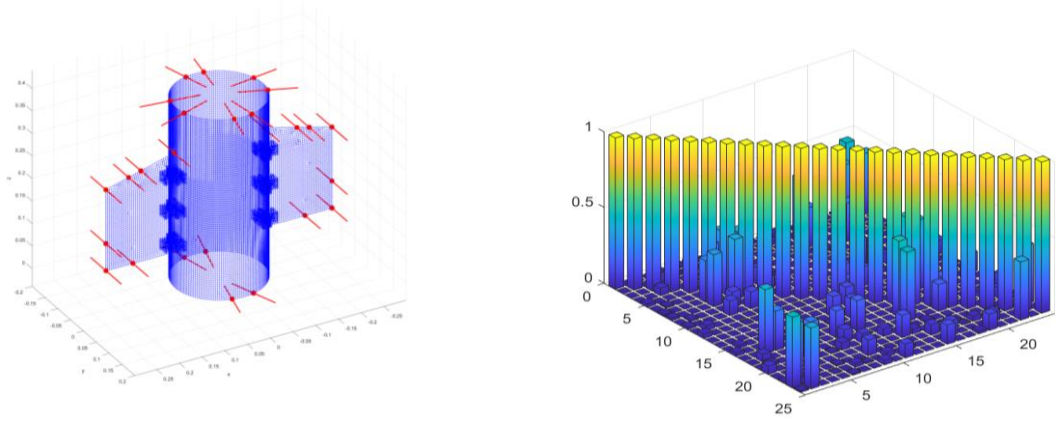

Figure 8: Sensor configurations by the sensor density approach and theirs AutoMAC. a) 20-sensor for M =18; b) 22-sensor configuration for $M = 22$; c) 26-sensor configuration for $M = 24$.

6 OSP for MAC and the condition number

Though the information entropy and FIM are valid objective functions for OSP, and this is rigorously proven, for test engineers these terms are not easy to comprehend. Typically, test engineers evaluate the informativeness of the sensor configuration by examining the mode shape matrix quality features such as the off-diagonal elements of the AutoMAC matrix and/or the condition number (CN) of the mode shape matrix $\kappa(\mathbf{L\Phi})$, see (1). The former is the measure of the mutual correlation between the mode shapes, and it, despite all its shortcomings [22], is perhaps one of the most popular tools of the experimental modal analysis. The latter indicates the quality of the pseudoinverse $(\mathbf{L\Phi})^{+}$ in terms of the sensitivity of the inverse problem to the measurement errors: a bigger CN may cause amplification of the measurement error when solving the inverse problem. The abovementioned inverse problem is employed in common engineering tools such as SEREP (System Equivalent Reduction Expansion Process) [23], orthogonality check [24] and virtual sensing utilizing the Modal Decomposition and Expansion approach [25].

However, employing the off-diagonal elements of the AutoMAC matrix or the CN as the objective function is rather difficult. Whilst adding an extra sensor *at any point* of the test object *always* increases the determinant of FIM (as it follows from Proposition 1 proven in [4], p.930), this is not the case for the two former features. Adding a sensor at any point of the test object can "worsen" the AutoMAC matrix and increase the CN. Appendix 1 illustrates this with a simple example.

When solving an OSP problem by maximizing the determinant of FIM, we do not directly control the AutoMAC matrix and the CN, however, the experience shows that they often converge to reasonable numbers. However, if the results are not satisfactory, one can consider multi-objective optimization. Papadimitriou in [15] suggested the Pareto approach to include other objectives to the OSP problem. The presented paper suggests extending the sensor density method via adding extra constraints to the optimization (3).

First, one can extend (3) by setting a constraint on the condition number:

$$\kappa(\mathbf{P\Phi}) \leq \kappa^{*}, \tag{8}$$

where κ^{*} is the requested condition number of the mode shape matrix. Figure 9a shows the sensor design and the corresponding AutoMAC matrix for $\kappa^{*} = 6$. Compared with the initial 16-sensor design generated without the constraint (Figure 5d), now the algorithm converges to a 19-sensor design, with the condition number improved from 9.3 to 6.2. The optimization takes more iterations as the algorithm needs to balance between maximizing the objective function and keeping the constraint fulfilled; the convergence history has a typical sawtooth shape. The convergence histories for both cases are shown in Figure 9b.

As was mentioned before, due to the approach the final sensor system design is generated (5), the final condition number may slightly differ from the requested one.

Along with the CN constraint, it is possible to introduce a constraint related to the off-diagonal terms of the AutoMAC matrix. There are different constraint formulations such as

- constraining the value of the specific element of the AutoMAC matrix. This is a good choice when a "problematic" element of the matrix is identified, which needs to be improved.
- constrain the biggest element of the AutoMAC. This choice can cause a problem when two or more elements of the AutoMAC are of approximately the same values, and the optimization routine can be confused by switching between them.
- constrain the mean of the off-diagonal elements. In this case, the danger is that the optimization routine can leave one of the elements relatively larger than the others while keeping the mean below the set limit.

a)

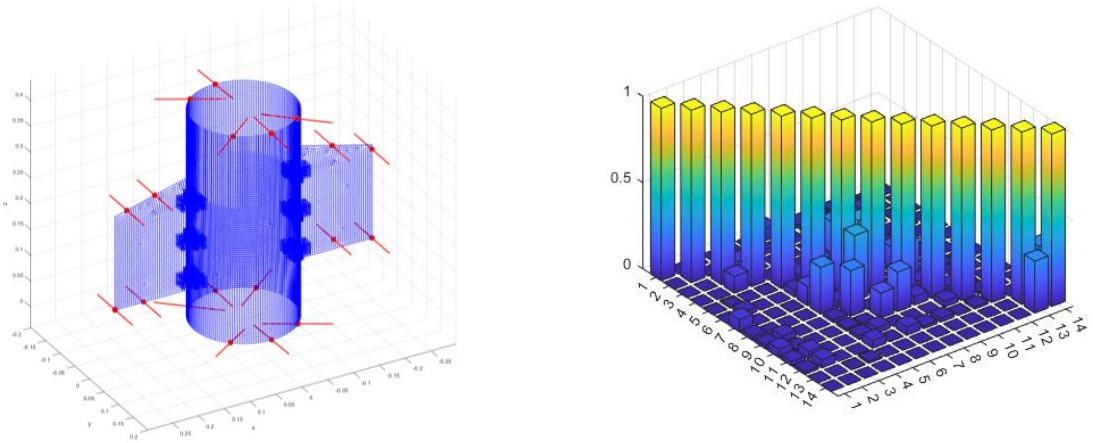

b)

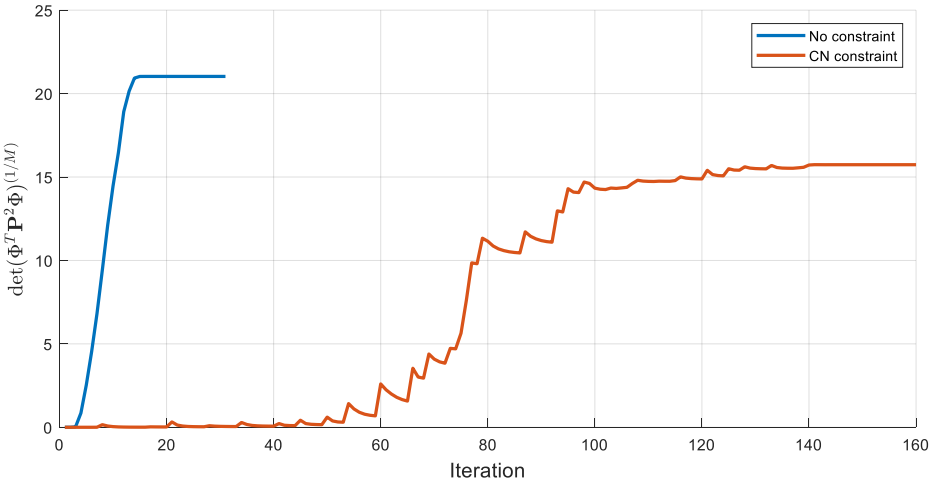

Figure 9: a) The 19-sensor configuration optimized for low condition number; b) corresponding convergence history (red) vs. the convergence history without the CN constraint.

An example of the first constraint is given below. Without setting any constraints, the design shown in Figure 5d is obtained. Examining the AutoMAC matrix, it was identified that the correlation between the 7th and 8th modes is too high, and the corresponding element of the matrix is 0.44. As the natural frequencies of the two modes are close, the high mode shape correlation can cause problems with the stabilization of the corresponding poles when using the stabilization diagram in modal analysis.

The optimization algorithm was re-set to constrain the problematic element to 0.3. The resulting 16-sensor design and the corresponding AutoMAC matrix are presented in Figure 10, where the correlation problem between the 7th and 8th modes is solved at the expense of worsening the objective function.

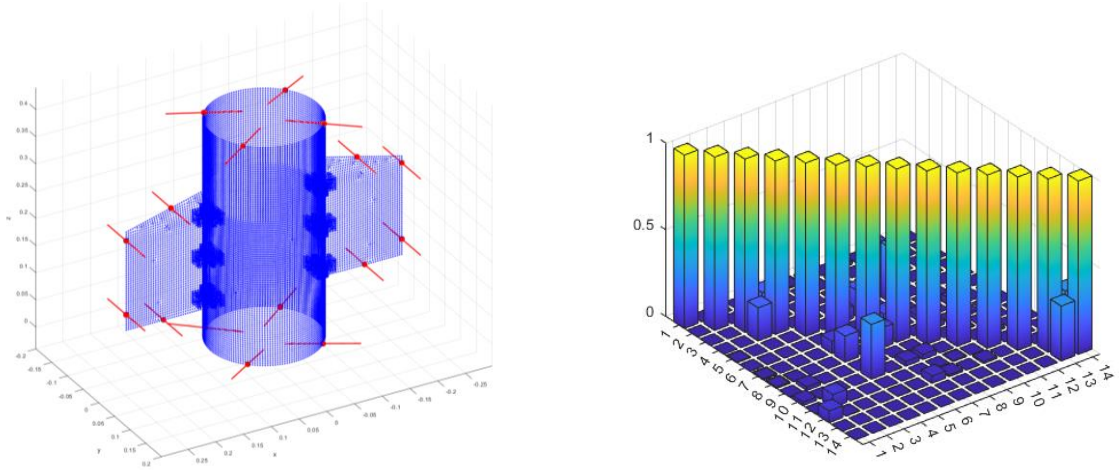

Figure 10: The 19-sensor configuration optimized to reduce the correlation between modes 7 and 8.

Conclusion

The paper introduces a sensor-density approach that allows relaxation of the binary optimization problem typical in solving the optimal sensor placement problem. As the objective function for OSP, the study employs the classical formulation, namely maximization of the determinant of the Fisher Information Matrix, which leads to the sensor configuration minimizing the uncertainty in the experimental model parameter estimation. The paper compares the results of the suggested approach with the conventional backward sequential sensor placement algorithm.

The paper attempts to represent the view of a practicing test engineer and extends the OSP to the traditional characteristics of the sensor configuration such as the AutoMAC matrix and the condition number of the mode shape matrix.

The paper also discusses the choice of the optimal number of sensors and the use of monoaxial sensors on complex 3D structures. For the latter case, the orientation of sensors is addressed, and the idea of principal measurement directions is suggested.

Acknowledgments

The work is supported by the Danish Energy Agency through the Energy Technology Development and Demonstration Program (EUDP), Grant No. 64021-1031. The supported project is named BLATIGUE-2: Fast, Smart and Efficient Fatigue Testing of Large Wind Turbine Blades.

References

[1] E. Balmès, “Orthogonal Maximum Sequence Sensor Placements Algorithms for modal tests, expansion and visibility,” in *International Modal Analysis Conference*, 2005, pp. 1–10.

[2] Kammer Daniel C., “Sensor Placement for On-orbit Modal Identification and Correlation of Large Space Structures,” *Journal of Guidance, Control, and Dynamics*, vol. 14, no. 2, pp. 251–259, 1991.

[3] Y.-T. Shih, A. C. Lee, and J.-H. Chen, “SENSOR AND ACTUATOR PLACEMENT FOR MODAL IDENTIFICATION,” *Mechanical Systems and Signal Processing*, vol. 12, no. 5, pp. 641–659, 1998.

[4] C. Papadimitriou, “Optimal sensor placement methodology for parametric identification of structural systems,” *Journal of Sound and Vibration*, vol. 278, no. 4–5, pp. 923–947, Dec. 2004, doi: 10.1016/j.jsv.2003.10.063.

[5] J. Zhang, K. Maes, G. de Roeck, E. Reynders, C. Papadimitriou, and G. Lombaert, “Optimal sensor placement for multi-setup modal analysis of structures,” *Journal of Sound and Vibration*, vol. 401, pp. 214–232, Aug. 2017, doi: 10.1016/j.jsv.2017.04.041.

[6] A. Mendler, M. Döhler, and C. E. Ventura, “Sensor placement with optimal damage detectability for statistical damage detection,” *Mechanical Systems and Signal Processing*, vol. 170, May 2022, doi: 10.1016/j.ymssp.2021.108767.

[7] W. Ostachowicz, R. Soman, and P. Malinowski, “Optimization of sensor placement for structural health monitoring: a review,” *Structural Health Monitoring*, vol. 18, no. 3. SAGE Publications Ltd, pp. 963–988, May 01, 2019. doi: 10.1177/1475921719825601.

[8] T. Ercan and C. Papadimitriou, “Optimal sensor placement for reliable virtual sensing using modal expansion and information theory,” *Sensors*, vol. 21, no. 10, May 2021, doi: 10.3390/s21103400.

[9] A. Mehrjoo, M. Song, B. Moaveni, C. Papadimitriou, and E. Hines, “Optimal Sensor Placement for Parameter Estimation and Virtual Sensing of Strains on an Offshore Wind Turbine Considering Sensor Installation Cost,” *Mechanical Systems and Signal Processing* , vol. 169, 2022.

[10] C. Papadimitriou and G. Lombaert, “The effect of prediction error correlation on optimal sensor placement in structural dynamics,” *Mechanical Systems and Signal Processing*, vol. 28, pp. 105–127, Apr. 2012, doi: 10.1016/j.ymssp.2011.05.019.

[11] H. B. Kim and Y. S. Park, “SENSOR PLACEMENT GUIDE FOR STRUCTURAL JOINT STIFFNESS MODEL IMPROVEMENT,” *Mechanical Systems and Signal Processing*, vol. 11, no. 5, pp. 651–672, Sep. 1997, doi: 10.1006/MSSP.1997.0108.

[12] Yao Leehter, Sethares William A., and Kammer Daniel C., “Sensor Placement for On-Orbit Modal Identification via a Genetic Algorithm,” *AIAA Journal*, vol. 31, no. 10, pp. 1922–1928, 1993.

[13] H. Sun and O. Büyüköztürk, “Optimal sensor placement in structural health monitoring using discrete optimization,” *Smart Materials and Structures*, vol. 24, no. 12, Nov. 2015, doi: 10.1088/0964-1726/24/12/125034.

[14] H. An, B. D. Youn, and H. S. Kim, “A methodology for sensor number and placement optimization for vibration-based damage detection of composite structures under model uncertainty,” *Composite Structures*, vol. 279, Jan. 2022, doi: 10.1016/j.compstruct.2021.114863.

[15] C. Papadimitriou, “Pareto optimal sensor locations for structural identification,” *Computer Methods in Applied Mechanics and Engineering*, vol. 194, no. 12–16, pp. 1655–1673, Apr. 2005, doi: 10.1016/j.cma.2004.06.043.

[16] S. Joshi and S. Boyd, “Sensor selection via convex optimization,” *IEEE Transactions on Signal Processing*, vol. 57, no. 2, pp. 451–462, 2009, doi: 10.1109/TSP.2008.2007095.

[17] S. Cantero-Chinchilla, J. L. Beck, M. Chiachío, J. Chiachío, D. Chronopoulos, and A. Jones, “Optimal sensor and actuator placement for structural health monitoring via an efficient convex cost-benefit optimization,” *Mechanical Systems and Signal Processing*, vol. 144, p. 106901, Oct. 2020, doi: 10.1016/J.YMSSP.2020.106901.

[18] P. Bhattacharyya and J. L. Beck, “Exploiting Convexification for Bayesian Optimal Sensor Placement by Maximization of Mutual Information,” *Structural Control Health Monitoring*, vol. 27, no. 10, Jun. 2020, [Online]. Available: http://arxiv.org/abs/1906.05953

[19] C. Papadimitriou, J. L. Beck, and S.-K. Au, “Entropy-Based Optimal Sensor Location for Structural Model Updating,” *Journal of Vibration and Control*, vol. 6, pp. 781–800, 2000.

[20] K. Svanberg, “The method of moving asymptotes—a new method for structural optimization,” *International Journal for Numerical Methods in Engineering*, vol. 24, no. 2, 1987, doi: 10.1002/nme.1620240207.

[21] M. I. Friswell and R. Castro-Triguero, "Clustering of sensor locations using the effective independence method," *AIAA Journal*, vol. 53, no. 5, pp. 1388–1390, 2015, doi: 10.2514/1.J053503.

[22] Allemang R.J., "The modal assurance criterion - Twenty years of use and abuse," *Sound & Vibration*, vol. 37, no. 8, pp. 14–23, 2003.

[23] J. O'Callahan, P. Avitabile, and R. Riemer, "SYSTEM EQUIVALENT REDUCTION EXPANSION PROCESS (SEREP)," in *International Modal Analysis Conference (IMAC)*, 1989, pp. 29–37.

[24] Michael L. Mains, "Orthogonality for Modal Vector Correlation: The Effects of Removing Degrees-of-Freedom," in *Topics in Model Validation and Uncertainty Quantification*, vol. 5, Todd Simmermacher, Scott Cogan, Babak Moaveni, and Costas Papadimitriou, Eds. Springer New York, 2013.

[25] A. Iliopoulos, R. Shirzadeh, W. Weijtjens, P. Guillaume, D. van Hemelrijck, and C. Devriendt, "A modal decomposition and expansion approach for prediction of dynamic responses on a monopile offshore wind turbine using a limited number of vibration sensors," *Mechanical Systems and Signal Processing*, vol. 68–69, pp. 84–104, Feb. 2016, doi: 10.1016/J.YMSSP.2015.07.016.

Appendix

Figure 11a displays the first two mode shapes of a simply supported uniform beam of a unit length instrumented with three evenly spaced sensors denoted by the black dots. The dotted lines show the mode shapes at the observed DOFs. Next to the figure, the values of the determinant of FIM, the condition number of the mode shape matrix and the off-diagonal element of the AutoMAC matrix are shown.

In Figure 11b, an extra sensor is added at position 0.375 and the mode shape matrix features are displayed. As it follows from Proposition 1 in [4], the determinant of the FIM increased as the number of sensors increased. However, the off-diagonal element of the AutoMAC matrix, which was "perfect" before, became worse. Same can be said about the condition number: with three sensors, the condition number was "perfect" but the number of sensors increase makes it worse.

a)

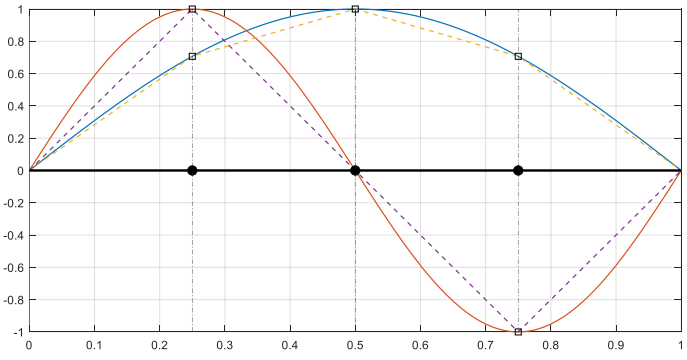

$\det(\mathbf{\Phi}^T\mathbf{L}^T\mathbf{L}\mathbf{\Phi}) = 4;$

$\kappa(\mathbf{L}\mathbf{\Phi}) = 1;$

$\text{AutoMAC}_{12} = 0$

b)

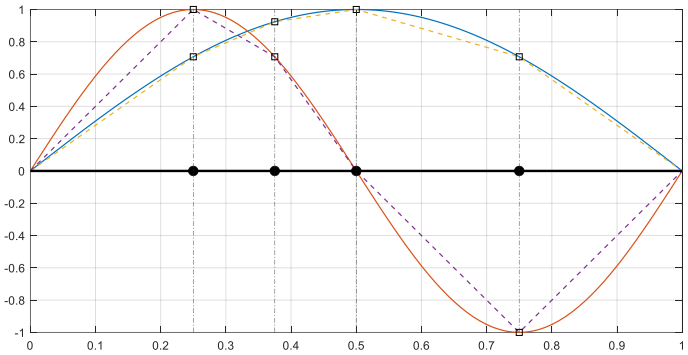

$\det(\boldsymbol{\Phi}^T\mathbf{L}^T\mathbf{L}\boldsymbol{\Phi}) = 6.71;$

$\kappa(\mathbf{L}\boldsymbol{\Phi}) = 1.29;$

$\text{AutoMAC}_{12} = 0.06$

Figure 11: Illustration of how the sensor count increase may worsen the features of the mode shape matrix.

Nomenclature

OSP	Optimal Sensor Placement
DOF	Degree-of-freedom
N	Number of DOFs in the numerical model
N_o	Number of the observed DOFs
M	Number of taken into account modes
$\boldsymbol{\Phi}$	Mode shapes matrix
$\mathbf{L}$	Observation matrix
$\mathbf{Q}$	Fisher Information Matrix, FIM
$\boldsymbol{\delta}$	Sensor configuration vector, discrete formulation
$\boldsymbol{\rho}$	Sensor configuration vector, sensor-density formulation
$\kappa(\mathbf{A})$	Condition number of a matrix $\mathbf{A}$